frontiers in Veterinary Science

TYPE Case Report
PUBLISHED 03 June 2026
DOI 10.3389/fvets.2026.1778231

Check for updates

OPEN ACCESS

EDITED BY
Nedzad Hadziomerovic,
University of Sarajevo,
Bosnia and Herzegovina

REVIEWED BY
Gabriele Gradner,
University of Veterinary Medicine Vienna,
Austria
Mohammed Messaoudi,
Ecole Normale Supérieure de Kouba,
Algeria

*CORRESPONDENCE
Kalman Czeibert
czeibertk@gmail.com

RECEIVED 30 December 2025
REVISED 12 May 2026
ACCEPTED 18 May 2026
PUBLISHED 03 June 2026

CITATION
Pajor C and Czeibert K (2026) Case Report: Dorsal stabilization of an occipito-atlanto-axial malformation in a Miniature Dachshund using 3D planning and a patient-specific titanium implant. *Front. Vet. Sci.* 13:1778231.
doi: 10.3389/fvets.2026.1778231

Case Report: Dorsal stabilization of an occipito-atlanto-axial malformation in a Miniature Dachshund using 3D planning and a patient-specific titanium implant

Csaba Pajor[1,2] and Kalman Czeibert[3]*

[1]Vac Veterinary Clinic and Hospital, Vac, Hungary, [2]PajorVet Bt, Vac, Hungary, [3]LimesVet Fiftyfive Ltd., Budapest, Hungary

Introduction: The craniocervical junction can be affected by various congenital or acquired disorders in dogs. When the normal alignment of occipital bone, atlas, and axis is altered, the resulting instability and spinal cord compression can cause mild to severe neurological signs. Occipito-atlanto-axial malformation (OAAM) is a relatively rare craniocervical junction disorder that may require surgical intervention to stabilize the bones and resolve neurological signs. Because OAAM can present in different anatomical forms, individualized decision-making and surgical planning are recommended to treat the malformation and associated instability effectively.

Methods: A 5-month-old female Miniature Dachshund was referred for cervical pain and progressive gait abnormalities with proprioceptive ataxia. Neurological examination was consistent with C1–C5 myelopathy. Magnetic resonance imaging (MRI) confirmed craniocervical spinal cord compression, and computed tomography (CT) identified severe C1 vertebral malformation, flattened occipital condyles, aplasia of the dens, and subluxation at the atlanto-occipital and atlanto-axial joints. CT-based virtual surgical planning was performed to create a patient-specific drilling guide and a 3D-printed customized Grade-23 titanium locking plate. Surgery was performed via a dorsal approach and included partial dorsal arch resection of the atlas and partial resection of the spinous process of the axis, followed by drilling at predefined positions, trajectories, and depths for screw placement. The implant was fixed to the occiput-atlas-axis complex using ten 2.4 mm titanium locking screws.

Results: Postoperative radiographs confirmed proper implant positioning and alignment, and no intraoperative or postoperative complications were observed. Neurological status did not deteriorate, and progressive improvement was noted from the second postoperative week. At 13 months, the dog had normal gait and spinal reflexes, showed no signs of pain or neurological deficits, and follow-up radiographs confirmed stable positioning of the implant and screws without evidence of loosening.

Discussion: Considering the postoperative outcome and other available techniques, this case supports the feasibility of dorsal stabilization of the craniocervical junction. Careful preoperative 3D planning may help identify fixation points and drilling trajectories (particularly when safe corridors are limited), thereby enhancing the surgical safety and enabling the use of a patient-specific biocompatible titanium plate for the fixation.

KEYWORDS
3D planning, atlantoaxial instability, craniocervical junction, occipito-atlanto-axial malformation (OAAM), patient-specific implant, veterinary neurosurgery, virtual surgical planning

Introduction

Occipito-atlanto-axial malformation is a rare but clinically important disorder in dogs that can be classified among craniocervical junction (CCJ) disorders. The CCJ is an anatomically and biomechanically linked unit composed of the occipital bone, the atlas (C1), and the axis (C2) as well as their associated ligaments (1). Its stability is essential for protecting the medulla oblongata and the spinal cord. Marino et al. (2) introduced the term craniocervical junction abnormality (CJA) to address congenital developmental disorders affecting the CCJ. According to their classification, the term CJA includes a group of disorders such as Chiari-like malformation (CLM), atlanto-occipital instability or dislocation (AOI/AOD), atlantoaxial instability (AAI), occipito-atlanto-axial malformation (OAAM), and atlanto-occipital overlapping (AOO). Among these conditions, AAI is the most common neurological disorder, predominantly affecting young dogs from toy and small breeds (1, 3–5). CCJ instability may develop due to underlying abnormalities such as aplasia or hypoplasia of the dens, malossification between the dens and the axis, dorsal angulation of the dens, or incomplete ossification of the atlas (1, 6). It can also have a traumatic origin, especially when the cranio-cervical and intervertebral ligamentous attachments are injured. Clinical signs can range from mild to severe pain and cervical hyperesthesia to ataxia or non-ambulatory tetraparesis, and in severe cases, respiration may also be affected (1, 3, 7, 8).

Due to the dynamic nature of the OAAM, surgical treatment is generally recommended, as in AAI. Commonly applied methods include a ventral approach to the craniocervical region with placement of pins or screws into the bones (9–12), and fixation may be augmented using polymethylmethacrylate (PMMA) (13–17). Other techniques treating AOI and AAI include different wiring methods, anchoring the atlas to the axis (18–21), to the occipital condyle (22), or to the zygomatic arch (23), anchoring the axis to the occipital bone (24), or placing non-absorbable sutures into the dorsal muscles over the CCJ (25). A recent publication presented a dorsal cemented technique with screws and PMMA to fix C1 and C2 (26). A study also described an indirect reduction technique using over-distraction for cases with AAI (27). These methods can stabilize the bones, but complication rates may be clinically relevant, especially in small breeds, where bone thickness is limited and accidental drilling and screw malposition can lead to bleeding, or neurological deficits. Retrospective studies describe an overall favorable outcome but also mention major adverse events in a minority of cases, highlighting implant-associated and perioperative risks (28, 29). Recent advances focus on improving surgical accuracy during drilling and screw placement and on utilizing customized implants. Since drilling trajectories can be planned from computed tomography (CT) data with higher precision than freehand techniques, optimal positions and angles can be identified, and 3D-printed guides can enhance intraoperative safety (30–32). Patient-specific approaches also enable implant manufacturing using traditional computer numerical control (CNC) methods. Patient-specific implants may be particularly useful for complex CCJ disorders when standard implants do not conform to severe osseous malformation, or when screw trajectory options are limited. Prior case studies described successful stabilization of atlanto-axial and OAAM disorders using ventral fixation, including custom-made and 3D-printed locking plates (33–35).

We report the case of a Miniature Dachshund with OAAM and concurrent AOD/AAI resulting in dynamic instability and dorsal compression treated using CT-based virtual surgical planning and a dorsally fixed customized titanium implant.

Case description

Preoperative examination

A 5-month-old female Miniature Dachshund was referred to the Vac Veterinary Clinic and Hospital in early 2025 for progressively worsening gait abnormalities and suspected AAI. Neurological examination revealed proprioceptive ataxia affecting all four limbs, and excessive claw wear was present on all limbs. Spinal reflexes showed upper motor neuron (UMN) signs in all four limbs, and the dog had severe neck pain during manipulation (flexion and extension) and palpation. Findings were consistent with a C1–C5 myelopathy with marked cervical pain. Orthopedic examination confirmed bilateral Grade-I medial patellar luxation. Routine bloodwork (hematology and biochemistry) and abdominal ultrasonography were performed and revealed no abnormalities.

CT was performed (voltage: 120 kV, current: 250 mA, slice thickness: 0.6 mm, with bone kernel; GE Healthcare 16-slice CT scanner, Chicago, Illinois, United States) and identified a severe C1 cervical vertebral malformation (ventral arch positioned more dorsally with an altered angle compared to physiological alignment, and a rounded dorsal arch), aplasia of the dens, flattened occipital condyles, and subluxation of the atlanto-occipital and atlanto-axial joints. These were altogether indicating the presence of OAAM. Despite visible AOD, no cerebellar compression was observed and the McRae line was not crossed by the atlas (36–38). The caudal part of the arcus dorsalis was tilted below the spinous process and dorsal arch of the axis (Figure 1A). T2-weighted MR imaging (field strength: 0.25 T, repetition time: 2020 ms, echo time: 90 ms; Vet-MR Grande 2019, Esaote, Italy) confirmed spinal cord compression and revealed a greater degree of ventral dislocation of the caudal part of the dorsal arch of the atlas than was visible on CT images (Figure 1B).

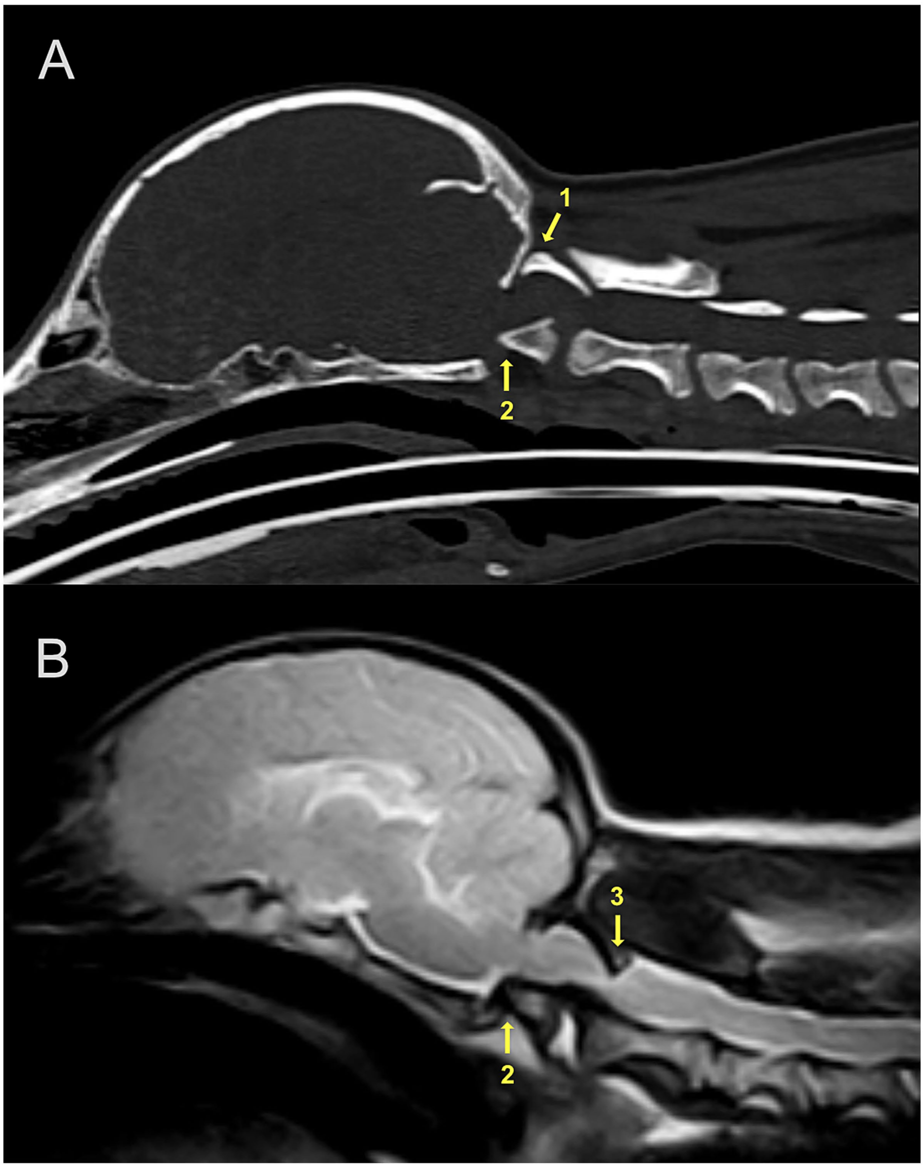

FIGURE 1
Diagnostic imaging of the craniocervical region. **(A)** Sagittal CT image (bone kernel) showing atlanto-occipital dislocation, atlantoaxial subluxation, and dens aplasia. **(B)** Sagittal T2-weighted MR image showing atlanto-axial subluxation, dens aplasia, and C1–C2 dorsal spinal cord compression. (1) Dorsal displacement of the atlas, dorsal arch. (2) Dorsal displacement of the atlas, ventral arch. (3) Dorsal compression of the spinal cord due to the displacement of the atlas.

Surgical planning and manufacturing

To stabilize the occipital bone and the first two vertebrae, a customized implant was designed due to the patient-specific anatomical situation. A neck bandage was applied to stabilize the head and neck until surgical intervention could be performed. First, a 3D model was created from the CT DICOM series using 3D Slicer[1] (39). The refined mesh was also colorized to map the bone thickness on the cranium, atlas, and axis (Figures 2A–D). This was used to identify fixation points while minimizing the possibility of iatrogenic damage and ensuring adequate bicortical distance for the planned screws.

Based on this evaluation, a ventral approach was discarded due to the thin basioccipital bone at the intended fixation site (average thickness <2.5 mm), which was considered insufficient for secure screw placement, and because dorsal compression caused by caudoventral tilting of the dorsal arch of the atlas was intended to be addressed. Therefore, the feasibility of a dorsal approach was assessed. The model showed that adjacent to the external occipital protuberance the skull was sufficiently thick to allow implant fixation while accounting for the underlying venous sinuses (confluence of sinuses and transverse sinuses). Multiple design variations were created until the implant was refined for manufacturing. The final implant was planned to be fixed with titanium locking screws, with screw lengths determined during surgical planning. A total of ten locking screws were planned: five in the caudal part of the skull, two dorsoventrally through the atlas (at the root of the ala atlantis), and three through the spinous process of the axis (Figure 2E). A drilling guide was also designed to be positioned on the target bone and determine the position, angle, and depth of drilling channels,

1 https://www.slicer.org

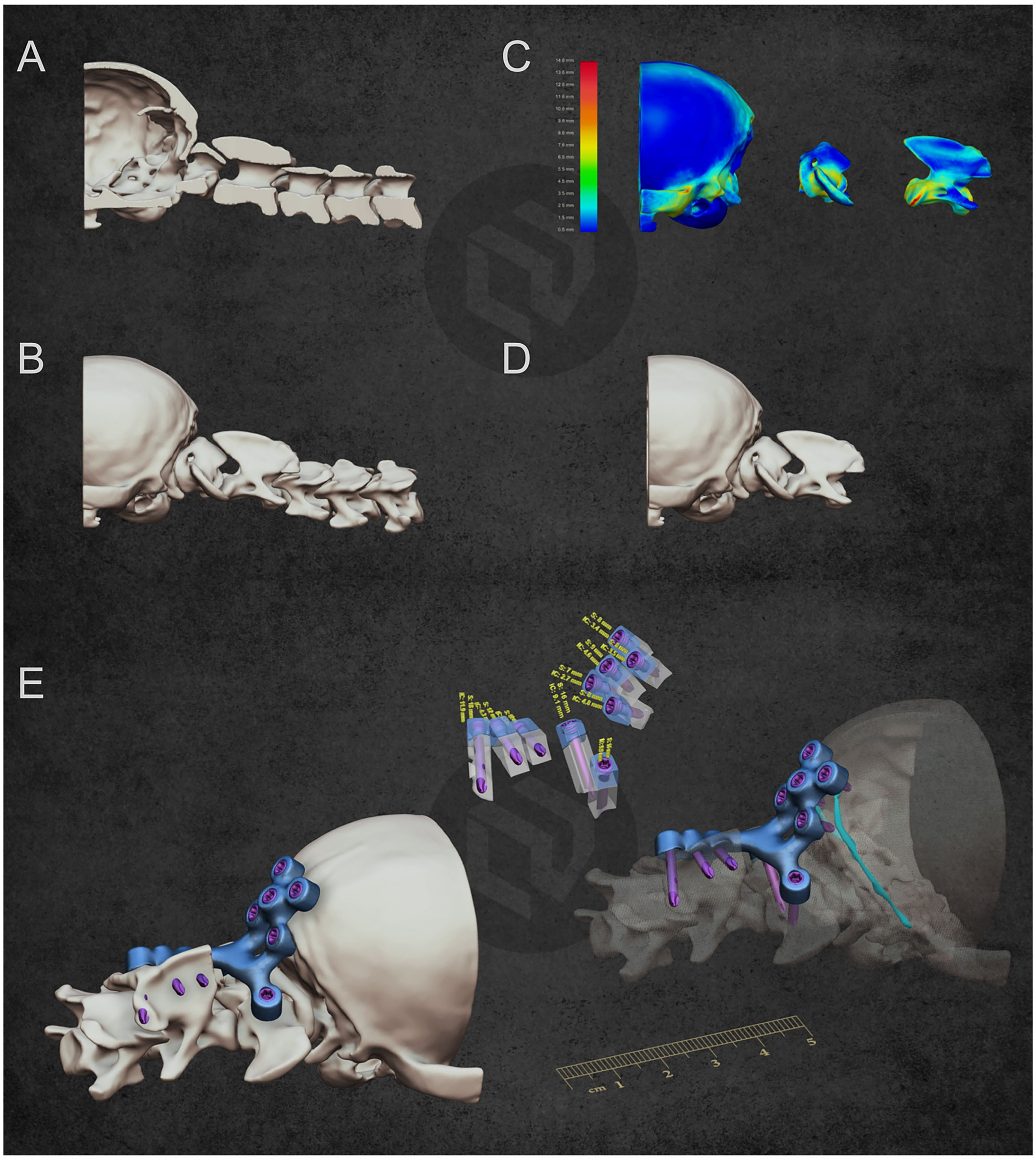

FIGURE 2
3D-visualization of the bones and surgical planning of the implant. **(A)** Right half of the caudal part of the skull and the first five cervical vertebrae. **(B)** Surface model of the craniocervical region. **(C)** Thickness mapping onto the cranium and the first two cervical vertebrae. **(D)** Caudal cranium with the atlas and axis. Link to the interactive 3D model: https://skfb.ly/ptAur. **(E)** On the right bones are shown with semitransparent color, the implant in blue, screws in purple, and the transverse sinus in light blue. The middle shows adjacent bone and implant areas at the screw locations, including total screw length, and bicortical distances. On the left, the implant and screws are shown with non-transparent bone models. Link to the interactive 3D model: https://skfb.ly/pETR6.

helping maintain a safe distance from the vertebral canal and major intracranial vessels.

Reference bone models and drilling guides were printed using a Stratasys J5 printer (Stratasys Ltd., Germany) with acrylate-based photopolymer resins, while the customized implant was manufactured by direct metal laser sintering (DMLS) using an SLM125HL machine (Nicon-SLM Solutions, Germany) from medical Grade-23 titanium alloy (Ti-6Al-4 V ELI). Internal threads to match the 2.4 mm locking screw head threads were formed using a CNC machine (Robodrill α-D21LIB5ADV+, Fanuc, Japan) during metal postprocessing, which also included acid etching and polishing (Figures 3A–C). All 3D-printed models (implant, guides, and bone models) were sterilized using an autoclave sterilizer (Gemmy SA-300H, Gemmy Industrial Corp., Taiwan) to ensure surgical sterility. Guide fit was verified on the printed bone model after sterilization.

Surgery

Surgery was performed on 22 March 2025. Anesthesia was conducted according to the principles of balanced, multimodal anesthesia (40). Premedication consisted of gabapentin (30 mg/kg PO) administered 2 h before anesthesia, combined with methadone (0.5 mg/kg IM). After intravenous catheter placement in the cephalic vein (22 G), general anesthesia was induced with propofol administered to effect (3*1 mg/kg IV), followed by intubation using a 5.5 mm internal diameter endotracheal tube. Anesthesia was maintained with isoflurane in

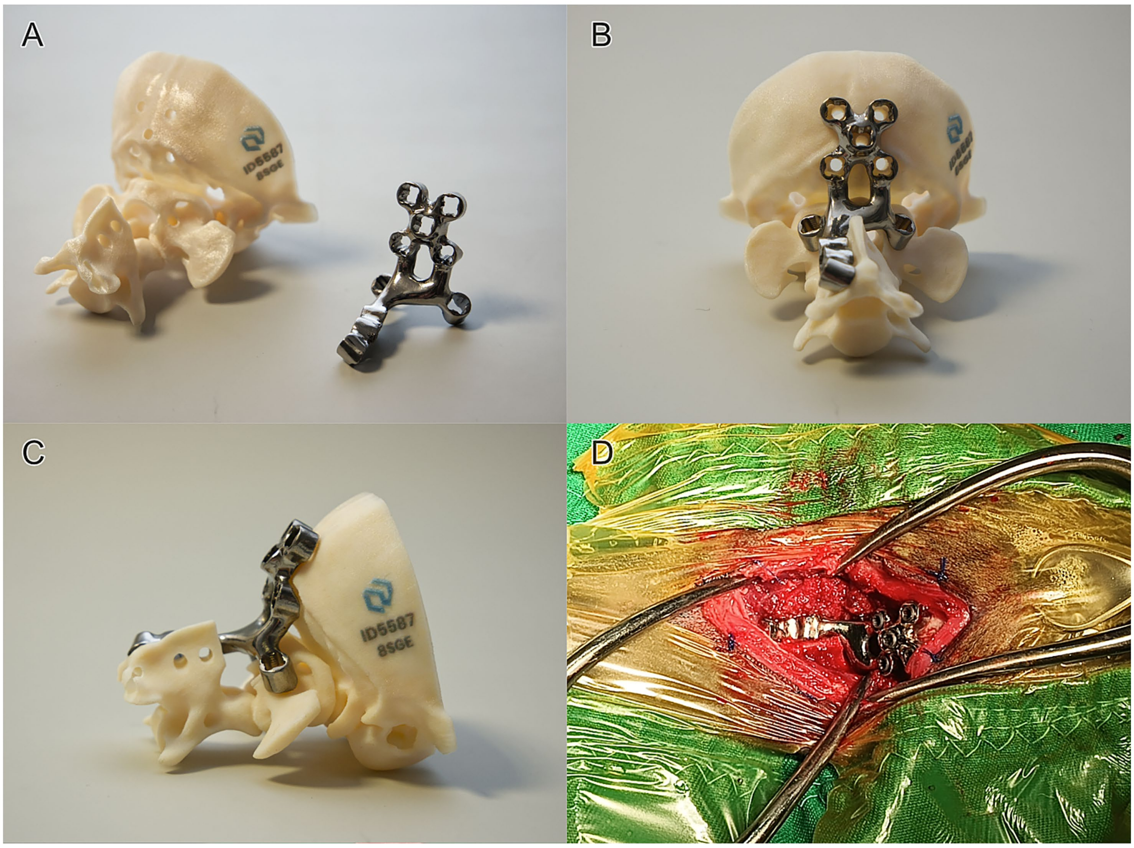

FIGURE 3
The 3D-printed titanium implant pre- and intraoperatively. **(A–C)** The implant with the 3D-printed bone model. **(A)** Right caudolateral view. **(B)** Caudal view. **(C)** Right view. **(D)** Implant fixed with locking screws in final position (top view).

oxygen to achieve an end-tidal concentration of approximately 0.8–1.5 vol%. Intraoperative analgesia was provided using a continuous rate infusion of fentanyl (5–10 μg/kg/h IV) combined with a low-dose ketamine CRI (0.3–0.6 mg/kg/h IV). Ringer's lactate was infused at 5 mL/kg/h. Maropitant (1 mg/kg IV) and cefazolin (30 mg/kg IV) were administered 30 min before surgery. Anesthesia was delivered using a Veterinary Anesthesia Machine Veta 5, and monitoring was performed using an ePM 12 VET patient monitoring system. Postoperative analgesia was provided using a multimodal approach, consisting of meloxicam (0.1 mg/kg IV) and methadone (0.5 mg/kg IM every 4 h).

The dog was positioned in sternal recumbency, and vacuum pillows were used to secure head position. The dorsal and dorsolateral cervical region and caudal head were clipped and aseptically prepared using alternating povidone-iodine and chlorhexidine scrubs, followed by sterile draping and application of an iodophor-impregnated adhesive incision drape. A dorsal midline skin incision was made from the external occipital protuberance to the level of the fourth cervical vertebra. The paraspinal muscles were separated atraumatically from the midline to expose the occipital bone and dorsal surfaces of the atlas and axis. Gelpi retractors maintained exposure. After cleaning the contact surface, the 3D-printed guide was placed onto the bones. The guide also helped determine the extent of resection of the spinous process (a few millimeters from its cranial end) of the axis to improve access to the caudal dorsal arch of the atlas. To relieve dorsal compression of the spinal cord, partial dorsal arch resection of C1 was performed using 1 mm and 2 mm Kerrison rongeurs, and the hypertrophied ligamentum flavum was also resected. Using the guide and implant, the vertebrae were stabilized in a neutral position (according to presurgical planning), avoiding ventral flexion, which is less preferred in this type of case (maintaining a neutral craniovertebral angle and avoiding iatrogenic malalignment). The guide was then used to create drilling channels in predefined positions using a 1.7 mm drill bit while the guide was held in place with manual pressure. Because the drill bit's body length had been measured beforehand, the guide design limited drilling depth, which was crucial to avoid brain injury. The customized titanium implant was placed and secured with 2.4 mm locking titanium screws (Figure 3D). The axis was stabilized with three screws (bicortical distances: 4.3, 5.5, and 11.9 mm), and the atlas with two screws at the base of the wings (bicortical distances: 9.1 and 9.9 mm). Because the occipital region had relatively small bicortical distances even at its thickest points, five screws were placed to aid fixation (bicortical distances: 2.7, 3.4, 3.5, 4.6, and 4.8 mm). Closure was achieved by apposition of the paraspinal musculature using a simple continuous pattern with monofilament absorbable suture (Ethicon PDS II Polydioxanone undyed monofilament absorbable suture, 3–0), followed by routine multilayer closure of subcutaneous tissue and skin.

Postoperative phase

Following surgery the dog was hospitalized for the first 48 h postoperatively under close monitoring, with cage restriction and leash

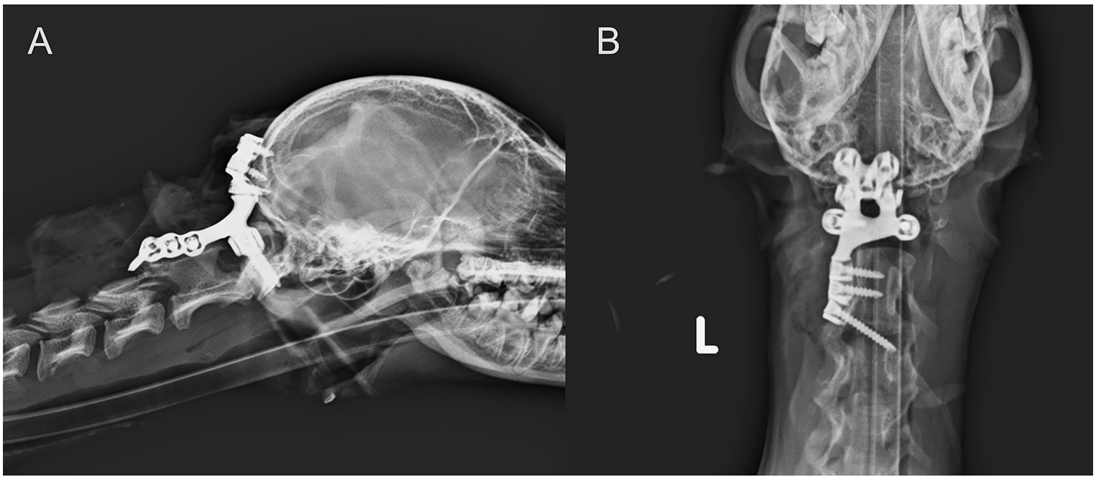

FIGURE 4
Postoperative radiographs of the craniocervical region. **(A)** Latero-lateral view. **(B)** Dorso-ventral view.

walking only. There was no deterioration in neurological status compared to the preoperative state, proprioceptive ataxia did not worsen, and no signs of neck pain were observed. Immediate postoperative radiographs demonstrated the implant and screws in their expected positions (Figures 4A,B). After hospitalization, the dog was discharged home, and a neck bandage was applied for 1 week. Medication was continued as follows: tramadol (4 mg/kg twice daily for 10 days), carprofen (2 mg/kg, once daily for 14 days), gabapentin (mg/kg, twice daily for 4 weeks) and vitamin B-complex (twice daily for 14 days, then once daily for the following 2 weeks). Sutures were removed 2 weeks postoperatively, at which time ataxia had slightly improved. Physiotherapy was offered, but the owner declined. At 4 weeks postoperatively, neurological examination revealed no lateralized gait abnormalities, no ataxia, normal spinal reflexes, physiological proprioception, and normal withdrawal reflexes. At 10 weeks postoperatively, no ataxia was present and no abnormal claw wear was observed. The neck was not painful on manipulation or palpation. Normal spinal reflexes were present in all four limbs, and the dog returned to normal function during walks and daily activities. Neurological status was summarized using the Modified Frankel Score (MFS) (Levine-derived 0–5 scale, with grade 3 subdivided into 3a/3b), in which grade 5 denotes normal gait with paraspinal hyperaesthesia, and grade 0 represents paraplegia/tetraplegia with loss of deep nociception (41, 42). Preoperatively, neurological status was MFS grade 4. By 1 month postoperatively, the dog has regained a clinically normal neurological status and was therefore outside the MFS grading system (since the MFS only describes neurologically compromised patients); this remained unchanged at the 13-month follow-up.

Discussion

OAAM can present with multi-joint deformities (arising from occipital malformation, abnormal load transfer, joint incongruity, or hypoplasia/aplasia of the dens), which may lead to instability and compressive myelopathy. This differs from isolated AAI because OAAM may involve more articulations and joint motion, may require a larger surgical approach, can limit the ability to achieve reduction using standard intraoperative positioning, and may carry a higher risk of surgical complications. Complications may arise from injury to the spinal cord, medulla oblongata, or encephalon. In addition, surgical approaches have been associated with complications such as pulmonary edema, hypothermia, dyspnea and apnea, worsened neurological status, dysphagia, regurgitation, aspiration, and breakage or migration of fixation (13, 14, 43, 44). Digital planning and 3D-printed guides may help maintain planned trajectories intraoperatively and reduce the risk of iatrogenic damage (45, 46). DMLS 3D-printing technology has also enabled the creation of fully customized medical implants from titanium or titanium alloys with complex geometries that may be difficult to manufacture using other techniques.

Rotter et al. (47) reported OAAM surgery using a ventral approach and a custom 3D-printed titanium implant with locking screws. In their case, the occipital bone was already fused to C1, therefore fixation targeted the atlanto-axial unit (47). Similarly, due to fusion of the occipital bone and atlas, Galban et al. (33) used two cortical screws to stabilize the bones. Kim et al. (48) described a Toy Poodle with AOD and AAI treated via ventral fixation combined with C1 facetectomy, using screws and wires with PMMA to stabilize the CCJ. Serrano et al. (34) reported a cat with OAAM treated using a customized implant, however, they used a ventral approach with dorsal decompression performed on different days, and a stainless steel implant with cortical screws. They reported postoperative respiratory signs, miosis, and opisthotonus, and performed revision surgery due to penetration of the cranial cavity by one screw (34). Another case study demonstrated that a 3D-printed skull implant can be securely attached to the occipital region to treat Chiari-like malformation (49). Multiple studies have shown that 3D-printed drilling guides can improve the accuracy of bicortical pedicle screw placement compared with freehand techniques (30, 32, 50). Recently, a customized 3D-printed plate was used for the treatment of atlantoaxial instability in three dogs (35). In these three cases, a dorsal surgical approach and stabilization of the atlas and axis were performed, initially using cortical screws and later locking screws to improve stability. The main difference compared to our case is that those dogs presented with atlanto-occipital overlapping concurrent with atlantoaxial instability. Consequently, the implant was designed to connect the first two cervical vertebrae while adding dorsal elevations to prevent cranial displacement of the atlas. In our case, the size of the foramen magnum was normal, and dorsal displacement of the atlas resulted in atlanto-occipital subluxation in addition to atlantoaxial instability. Therefore, stabilization of the atlanto-occipital joint was also required, requiring the fixation of the customized implant to the occipital bone near the inion.

Patient-specific planning was chosen in our case to address two common CCJ problems: (a) achieving safe screw trajectories in the vertebrae and skull, and (b) optimizing implant fit by designing the final contoured form, reducing intraoperative time traditionally required to contour plates. Recent reports support workflows combining patient-specific guides with PMMA or customized titanium plates in toy breeds (33, 51). Although these studies mainly address AAI rather than OAAM, the principle of improving trajectory accuracy and reducing intraoperative uncertainty translates to occipito-atlanto-axial disorders where safe placement and depth may depend on millimeters. The main advantages in this case included: (a) fixation of the neck in a neutral position, as planned preoperatively; (b) use of a dorsal approach to increase safety and reduce the chance of iatrogenic injury during surgical approach to the bones; (c) dorsal decompression in same sitting at the region where the dorsal arch of the atlas was displaced toward the vertebral canal; (d) avoidance of PMMA (thereby avoiding thermal injury and PMMA bulk in the cervical/occipital region and potentially reducing infection risk); (e) use of preoperative 3D-planning and thickness analysis to define optimal drilling position, direction, and depth; (f) customized implant shape to minimize the risk of fixation in a suboptimal alignment; (g) use of medical-grade biocompatible titanium alloy; and (h) postprocessing of the implant to accept standard surgical locking titanium screws, supporting time and cost efficiency. Because screw sizes were selected based on preoperative measurements, they could be prepared in advance, and because they were part of a standard set, intraoperative changes could be accommodated if needed.

Limitations of this case report include: (a) postoperative CT was not performed (owner declined), and only follow-up radiographs were obtained (but demonstrated stable implant alignment without evidence of loosening, and the dog remained clinically stable with progressive neurological improvement throughout follow-up); although postoperative CT would have been preferable to confirm screw trajectories and exclude subtle cortical breach, follow-up radiographs showed no displacement and no radiographic signs of lysis around the implant and screws; (b) 3D technology and customized solutions (particularly DMLS manufacturing) are not widely available and generally more expensive than standard techniques; (c) customized implant workflows require design and manufacturing time and are therefore not suitable for peracute cases when immediate stabilization is needed; (d) this present case report details one patient (due to the lower incidence of the OAAM compared to AAI) (1), (e) when feasible, biomechanical evaluation (e.g., finite element analysis) may be beneficial for assessing the stability of the virtual model, and (f) a dorsal approach may also be associated with muscle pain or seroma formation (however, these were not observed in this case, and the implant did not create clinically relevant prominence affecting welfare). Despite these limitations, based on intraoperative handling, follow-up examinations, and the dog's current clinical status, the outcome was favorable. Considering advances in veterinary and human surgery, it is likely that patient-specific planning and 3D technologies will become increasingly integrated in complex cases where safety and risk reduction are priorities.

Data availability statement

The original contributions presented in the study are included in the article/supplementary material, further inquiries can be directed to the corresponding author.

Ethics statement

Ethical approval was not required for the studies involving animals in accordance with the local legislation and institutional requirements because the procedures described were performed as part of standard veterinary clinical care. Written informed consent was obtained from the owners for the participation of their animals in this study. Written informed consent was obtained from the participant/patient(s) for the publication of this case report.

Author contributions

CP: Resources, Writing – original draft, Investigation, Validation, Project administration, Conceptualization, Supervision, Methodology, Writing – review & editing. KC: Project administration, Visualization, Supervision, Methodology, Writing – review & editing, Software, Investigation, Writing – original draft, Conceptualization, Resources, Validation.

Funding

The author(s) declared that financial support was not received for this work and/or its publication.

Acknowledgments

The authors would like to thank VetScan Ltd. for performing the diagnostic imaging, Renata Demeter for anesthesiology assistance, and the entire team of the Vac Veterinary Clinic and Hospital for their dedicated perioperative management.

Conflict of interest

KC was employed by LimesVet Fiftyfive Ltd.

The remaining author(s) declared that this work was conducted in the absence of any commercial or financial relationships that could be construed as a potential conflict of interest.

Generative AI statement

The author(s) declared that Generative AI was used in the creation of this manuscript. As the authors are not native English speakers, OpenAI's ChatGPT Plus (GPT-5.2) was used for English grammar and language refinement; all scientific content, interpretation, and conclusions are those of the authors.

Any alternative text (alt text) provided alongside figures in this article has been generated by Frontiers with the support of artificial intelligence and reasonable efforts have been made to ensure accuracy, including review by the authors wherever possible. If you identify any issues, please contact us.

Publisher's note

References

1. Cerda-Gonzalez S, Dewey CW. Congenital diseases of the craniocervical junction in the dog. *Vet Clin North Am Small Anim Pract*. (2010) 40:121–41. doi: 10.1016/j.cvsm.2009.10.001

2. Marino DJ, Loughin CA, Dewey CW, Marino LJ, Sackman JJ, Lesser ML, et al. Morphometric features of the craniocervical junction region in dogs with suspected Chiari-like malformation determined by combined use of magnetic resonance imaging and computed tomography. *Am J Vet Res*. (2012) 73:105–11. doi: 10.2460/ajvr.73.1.105

3. Stalin C, Gutierrez-Quintana R, Faller K, Guevar J, Yeamans C, Penderis J. A review of canine atlantoaxial joint subluxation. *Vet Comp Orthop Traumatol*. (2015) 28:1–8. doi: 10.3415/VCOT-14-05-0064

4. Sharp N, Wheeler S. *Small Animal Spinal Disorders*. 2nd ed. London: Mosby Ltd. (2004).

5. Shores A and Brisson BA, editors. *Current Techniques in Canine and Feline Neurosurgery*. Hoboken: Wiley-Blackwell (2017).

6. Watson AG, de Lahunta A, Evans HE. Morphology and embryological interpretation of a congenital occipito-atlanto-axial malformation in a dog. *Teratology*. (1988) 38:451–9. doi: 10.1002/tera.1420380508

7. Havig ME, Cornell KK, Hawthorne JC, McDonnell JJ, Selcer BA. Evaluation of non-surgical treatment of atlantoaxial subluxation in dogs: 19 cases (1992–2001). *J Am Vet Med Assoc*. (2005) 227:257–62. doi: 10.2460/javma.2005.227.257

8. Steffen F, Flueckiger M, Montavon PM. Traumatic atlanto-occipital luxation in a dog: associated hypoglossal nerve deficits and use of 3-dimensional computed tomography. *Vet Surg*. (2003) 32:411–5. doi: 10.1053/jvet.2003.50056

9. Progin A, Voumard B, Friker B, Forterre F. Biomechanical evaluation of two dorsal and two ventral stabilization techniques for atlantoaxial joint instability in toy-breed dogs. *Am J Vet Res*. (2021) 82:802–10. doi: 10.2460/ajvr.82.10.802

10. Jaggy A, Hutto VL, Roberts RE, Oliver JE. Occipitoatlantoaxial malformation with atlantoaxial subluxation in a cat. *J Small Anim Pract*. (1991) 32:366–72. doi: 10.1111/j.1748-5827.1991.tb00953.x

11. Wheeler SJ. Atlantoaxial subluxation with absence of the dens in a rottweiler. *J Small Anim Pract*. (1992) 33:90–3. doi: 10.1111/j.1748-5827.1992.tb01082.x

12. Shores A, Tepper LC. A modified ventral approach to the atlantoaxial junction in the dog. *Vet Surg*. (2007) 36:765–70. doi: 10.1111/j.1532-950X.2007.00334.x

13. Platt SR, Chambers JN, Cross A. A modified ventral fixation for surgical Management of Atlantoaxial Subluxation in 19 dogs. *Vet Surg*. (2004) 33:349–54. doi: 10.1111/j.1532-950X.2004.04050.x

14. Aikawa T, Shibata M, Fujita H. Modified ventral stabilization using positively threaded profile pins and Polymethylmethacrylate for atlantoaxial instability in 49 dogs. *Vet Surg*. (2013) 42:683–92. doi: 10.1111/j.1532-950X.2013.12016.x

15. Buks Y, Snelling SR, Yates GD. Ventral fixation of chronic atlanto-occipital luxation in a dog. *J Small Anim Pract*. (2011) 52:497–500. doi: 10.1111/j.1748-5827.2011.01100.x

16. Ferreira DRC, Dias LGG, Minto BW, Rocha TA, Malta CA, Conceição ME, et al. Biomechanical evaluation of four surgical techniques for ventral stabilization of the atlantoaxial joint in dogs. *Acta Cir Bras*. (2023) 38:e383223. doi: 10.1590/acb383223

17. Stout Steele MW, Hodshon AW, Hopkins AL, Tracy GM, Cohen ND, Kerwin SC, et al. Multi-center retrospective evaluation of screw and Polymethylmethacrylate constructs for atlantoaxial fixation in dogs. *Vet Surg*. (2016) 45:909–15. doi: 10.1111/vsu.12533

18. Forterre F, Zorgevica-Pockevica L, Precht C, Haenssgen K, Stein V, Düver P. Clinical evaluation of a new surgical augmentation technique for transarticular atlantoaxial fixation for treatment of atlantoaxial instability. *Animals*. (2023) 13:1780. doi: 10.3390/ani13111780

19. Han HJ, Kang J, Yoon HY. The use of a pin-screw-wire tie-in configuration for ventral stabilization of congenital atlantoaxial instability in a Yorkshire terrier. *Vlaams Diergeneeskd Tijdschr*. (2019) 88:219–225. doi: 10.21825/vdt.v88i4.16011

20. Kim D, Lee S, Kim G. Application of a modified dorsal wiring method in toy breed dogs with atlantoaxial subluxation. *In Vivo*. (2023) 37:247–51. doi: 10.21873/invivo.13074

21. Pujol E, Bouvy B, Omaña M, Fortuny M, Riera L, Pujol P. Use of the Kishigami atlantoaxial tension band in eight toy breed dogs with atlantoaxial subluxation. *Vet Surg*. (2010) 39:35–42. doi: 10.1111/j.1532-950X.2009.00613.x

22. Crane SW. Surgical management of traumatic atlanto-occipital instability in a dog. *Vet Surg*. (1978) 7:39–42. doi: 10.1111/j.1532-950X.1978.tb00577.x

23. Dolera M, Malfassi L, Bianchi C, Carrara N, Corbetta L, Finesso S, et al. Zygomatic arch-atlas wing stabilization in 5 dogs with atlanto-occipital dislocation. *J Vet Med Sci*. (2016) 78:963–70. doi: 10.1292/jvms.15-0421

24. Vedrine B, Maurin M. Dorsal surgical stabilisation using tension bands for treatment of traumatic atlanto-occipital instability in a cat. *Aust Vet J*. (2017) 95:469–73. doi: 10.1111/avj.12651

25. Sánchez-Masian D, Luján-Feliu-Pascual A, Font C, Mascort J. Dorsal stabilization of atlantoaxial subluxation using non-absorbable sutures in toy breed dogs. *Vet Comp Orthop Traumatol*. (2014) 27:62–7. doi: 10.3415/VCOT-13-01-0009

26. Tabanez J, Gutierrez-Quintana R, Kaczmarska A, José-López R, Nadal VG, Rotter C, et al. Evaluation of a novel dorsal-cemented technique for atlantoaxial stabilisation in 12 dogs. *Life*. (2021) 11:1039. doi: 10.3390/life11101039

27. Forterre F, Vizcaino Revés N, Stahl C, Gendron K, Spreng D. An indirect reduction technique for ventral stabilization of atlantoaxial instability in miniature breed dogs. *Vet Comp Orthop Traumatol*. (2012) 25:332–6. doi: 10.3415/VCOT-11-07-0107

28. Sanders SG, Bagley RS, Silver GM, Moore M, Tucker RL. Outcomes and complications associated with ventral screws, pins, and polymethyl methacrylate for atlantoaxial instability in 12 dogs. *J Am Anim Hosp Assoc*. (2004) 40:204–10. doi: 10.5326/0400204

29. Beaver DP, Ellison GW, Lewis DD, Goring RL, Kubilis PS, Barchard C. Risk factors affecting the outcome of surgery for atlantoaxial subluxation in dogs: 46 cases (1978–1998). *J Am Vet Med Assoc*. (2000) 216:1104–9. doi: 10.2460/javma.2000.216.1104

30. Elford JH, Oxley B, Behr S. Accuracy of placement of pedicle screws in the thoracolumbar spine of dogs with spinal deformities with three-dimensionally printed patient-specific drill guides. *Vet Surg*. (2020) 49:347–53. doi: 10.1111/vsu.13333

31. Hamilton-Bennett SE, Oxley B, Behr S. Accuracy of a patient-specific 3D printed drill guide for placement of cervical transpedicular screws. *Vet Surg*. (2018) 47:236–42. doi: 10.1111/vsu.12734

32. Guirguis P, Asanovic I, Beggs DS, Long SN. Retrospective analysis of custom 3D-printed drill guides and titanium plate use in spinal stabilization of eleven dogs. *Front Vet Sci*. (2024) 11:11. doi: 10.3389/fvets.2024.1491620

33. Galban EM, Gilley RS, Long SN. Surgical stabilization of an Occipitoatlantoaxial malformation in an adult dog. *Vet Surg*. (2010) 39:1001–4. doi: 10.1111/j.1532-950X.2010.00734.x

34. Aires Serrano C, Farré Mariné A, Luján Feliu-Pascual A. Ventral fixation and dorsal decompression of a complex occipitoatlantoaxial malformation using a custom-made plate in a cat. *JFMS Open Rep*. (2025) 11:20551169251328579. doi: 10.1177/20551169251328579

35. Guichard M, Sager F. Dorsal 3D-printed plate stabilisation of atlantoaxial instability associated with atlanto-occipital overlap in three dogs. *J Small Anim Pract*. (2026) 67:368–72. doi: 10.1111/jsap.70069

36. Takahashi F, Kouno S, Yamaguchi S, Hara Y. Evaluation of atlantooccipital overlapping and cerebral ventricle size in dogs with atlantoaxial instability. *J Vet Med Sci*. (2019) 81:229–36. doi: 10.1292/jvms.17-0553

37. Takahashi F, Hakozaki T, Kouno S, Suzuki S, Sato A, Kanno N, et al. Atlantooccipital overlapping and its effect on outcomes after ventral fixation in dogs with atlantoaxial instability. *J Vet Med Sci*. (2018) 80:526–31. doi: 10.1292/jvms.17-0438

38. Waschk MA, Vidondo B, Carrera I, Hernandez-Guerra AM, Moissonnier P, Plessas IN, et al. Craniovertebral junction anomalies in small breed dogs with atlantoaxial instability: a multicentre case-control study. *Vet Comp Orthop Traumatol*. (2019) 32:33–40. doi: 10.1055/s-0038-1675797

39. Fedorov A, Beichel R, Kalpathy-Cramer J, Finet J, Fillion-Robin JC, Pujol S, et al. 3D slicer as an image computing platform for the quantitative imaging network. *Magn Reson Imaging*. (2012) 30:1323–41. doi: 10.1016/j.mri.2012.05.001

40. Lamont LA, Grimm KA, Robertson S, Love L and Schroeder C, editors. *Veterinary Anesthesia and Analgesia, The 6th Edition of Lumb and Jones*. 6th ed. Hoboken: Wiley-Blackwell (2024).

41. Elliott RC, Moon C, Zeiler G, Lobetti R. Short-term clinical outcomes of 220 dogs with thoraco-lumbar disc disease treated by mini-hemilaminectomy. *J S Afr Vet Assoc*. (2020) 91:2008. doi: 10.4102/jsava.v91i0.2008

42. Levine GJ, Levine JM, Budke CM, Kerwin SC, Au J, Vinayak A, et al. Description and repeatability of a newly developed spinal cord injury scale for dogs. *Prev Vet Med*. (2009) 89:121–7. doi: 10.1016/j.prevetmed.2009.02.016

43. Schulz KS, Waldron DR, Fahie M. Application of ventral pins and polymethylmethacrylate for the management of atlantoaxial instability: results in nine dogs. *Vet Surg*. (1997) 26:317–25. doi: 10.1111/j.1532-950x.1997.tb01504.x

44. Thomas WB, Sorjonen DC, Simpson ST. Surgical management of atlantoaxial subluxation in 23 dogs. *Vet Surg*. (1991) 20:409–12. doi: 10.1111/j.1532-950X.1991.tb00348.x

45. Pijpker PAJ, Kraeima J, Witjes MJH, Oterdoom DLM, Vergeer RA, Coppes MH, et al. Accuracy of patient-specific 3D-printed Drill guides for pedicle and lateral mass screw insertion. *Spine*. (2021) 46:160–8. doi: 10.1097/BRS.0000000000003747

46. Marengo N, Colonna S, Bue EL, Pesaresi A, Saaid A, Allevi M, et al. Cervical pedicle screw placement with patient-specific 3D-printed guides: accuracy and safety in a clinical experience. *Eur Spine J*. (2025) 34:1248–55. doi: 10.1007/s00586-025-08679-2

47. Rotter C, Rusbridge C, Fitzpatrick N. Occipitoatlantoaxial malformation in a dog treated with a custom-made implant. *Vet Comp Orthop Traumatol*. (2020) 03:e170–6. doi: 10.1055/s-0040-1721030

48. Kim KB, Jeong JM, Jeon YJ, Jeong SM, Kim DH, Lee HB. C1 Facetectomy and ventral fixation of Occipitoatlantoaxial complex for concurrent congenital Atlanto-occipital dislocation and atlantoaxial instability in a toy poodle. *Animals*. (2024) 14:1886. doi: 10.3390/ani14131886

49. Colverde AS, Nicetto T, Falzone C. Occipital cranioplasty using customized titanium prosthesis yields successful outcome in association with foramen magnum decompression in dogs suffering by Chiari-like malformation. *Am J Vet Res*. (2022) 83:275–82. doi: 10.2460/ajvr.21.11.0178

50. Yu Y, Kang J, Kim N, Heo S. Accuracy of a patient-specific 3D-printed drill guide for placement of bicortical screws in atlantoaxial ventral stabilization in dogs. *PLoS One*. (2022) 17:e0272336. doi: 10.1371/journal.pone.0272336

51. Seon Y, Cho C, Jung C, Lim JH, Kim SY, Kang BJ. Atlantoaxial joint stabilization using patient-specific 3-D–printed drill guides and 3-D–printed titanium plates or polymethyl methacrylate is effective in toy-breed dogs. *Am J Vet Res*. (2024) 85:ajvr.24.02.0023. doi: 10.2460/ajvr.24.02.0023